

Dissipationless kinetics of one dimensional interacting fermions

I. V. Protopopov,^{1,2} D. B. Gutman,^{3,4} M. Oldenburg,¹ and A. D. Mirlin^{4,1,5}

¹ *Institut für Theorie der Kondensierten Materie and DFG Center for Functional Nanostructures, Karlsruhe Institute of Technology, 76128 Karlsruhe, Germany*

² *L. D. Landau Institute for Theoretical Physics RAS, 119334 Moscow, Russia*

³ *Department of Physics, Bar Ilan University, Ramat Gan 52900, Israel*

⁴ *Institut für Nanotechnologie, Karlsruhe Institute of Technology, 76021 Karlsruhe, Germany*

⁵ *Petersburg Nuclear Physics Institute, 188300 St. Petersburg, Russia.*

We study the problem of evolution of a density pulse of one-dimensional interacting fermions with a non-linear single-particle spectrum. We show that, despite non-Fermi-liquid nature of the problem, non-equilibrium phenomena can be described in terms of a kinetic equation for certain quasiparticles related to the original fermions by a non-linear transformation which decouples the left- and right-moving excitations. Employing this approach, we investigate the kinetics of the phase space distribution of the quasiparticles and thus determine the time evolution of the density pulse. This allows us to explore a crossover from the essentially free-fermion evolution for weak or short-range interaction to hydrodynamics emerging in the case of sufficiently strong, long-range interaction.

PACS numbers: 73.23.-b, 73.50-Td05.30.Fk, 73.21.Hb, 73.22.Lp, 47.37.+q

Understanding non-equilibrium phenomena is one of central themes in condensed matter physics. For Fermi-liquid systems (e.g. electrons in metals) such phenomena are conventionally described in the framework of a quantum kinetic equation for quasiparticle excitations. According to Landau Fermi-liquid theory, it has the same form as for weakly interacting particles up to a renormalization of parameters (effective mass, interaction constants, and scattering integral). This equation governs the evolution of a single-particle density matrix (characterizing the quasiparticle phase space distribution) and readily yields various physical observables¹⁻³.

For a variety of strongly interacting fermionic systems, the Fermi liquid theory (at least, in its standard form) is not applicable: interaction destroys the quasiparticle pole. In these cases one has to find an alternative way to describe transport and non-equilibrium phenomena. This is usually done by formulating effective theories in terms of some collective degrees of freedom. A famous realization of a non-Fermi-liquid state is provided by one-dimensional (1D) interacting fermions. This system is characterized by a strongly correlated ground state—Luttinger liquid (LL)⁴⁻⁸—which exhibits an infrared divergence of an electronic self-energy, eliminating the quasiparticle pole from the spectral function. This manifests itself in a power-law suppression of the tunneling (zero-bias anomaly) and indicates that quasiparticle excitations are ill-defined. A well-known tool for dealing with such correlated 1D systems is bosonization⁴⁻⁸. After linearization of the fermionic spectrum, it allows one to map the problem onto one of non-interacting bosons. For arbitrary distribution functions, the non-equilibrium bosonization yields results for LL correlation functions in terms of singular Fredholm determinants^{9,10}.

In this work we explore kinetics of interacting 1D fermions, having in mind the following model setup. Initially, a hump (or a dip) in a fermionic density is created

by an external potential. At time $t = 0$ the potential is switched off, and electronic pulses start to propagate to the right and to the left. The evolution of the electronic density as a function of time is measured. While experiments of this type are particularly natural in the context of cold atomic gases^{11,12}, we expect them to be feasible also for electronic systems. Since for a linearized spectrum the pulse moves without changing its form, a curvature of the single-particle spectrum is absolutely essential for the problem under consideration. Specifically, the curvature induces a tendency to an “overtake” of the pulse at a certain time t_c , thus making the pulse evolution for times $t > t_c$ a challenging problem¹³.

The non-linearity of a fermionic spectrum induces an interaction between bosonic collective modes¹⁴⁻²⁰, giving rise to a quantum hydrodynamic theory. Such “non-linear Luttinger liquids” arise in a variety of fermionic, bosonic, and spin system and have recently attracted a considerable attention^{21,22}.

A natural idea is to try to tackle the interaction between the bosonic modes perturbatively²³. As it turns out, the 1D character of the problem induces infrared singularities invalidating the naive perturbative expansion. The bosonized theory is treatable only in the limit of strong and long-ranged interaction, which justifies the saddle-point approximation, as was done in Ref.¹³ for Calogero model and in Ref.²⁴ for a generic interaction. Equations of motion obtained in this way can be viewed as Euler and continuity equation for an ideal fluid, and therefore the system is described by a non-dissipative classical hydrodynamics. Depending on the sign of the initial pulse, an interplay between non-linearity and dispersion leads to emergence of strong density oscillations or of solitons after the shock²⁴.

The problem has been also studied in the opposite limit of free fermions^{24,25}, where the evolution of Wigner function is described by a simple kinetic equation. For suf-

ficiently long times, $t > t_c$, a population inversion occurs, leading to density oscillations that can be viewed as Friedel-type oscillations between different Fermi edges.

Thus, the pulse evolution was analyzed in two opposite limits (no vs. strong long-range interaction) by different means (fermionic vs. bosonic), and within different physical pictures (inverted population vs. hydrodynamic waves). We now address this problem for an arbitrary interaction. By bosonizing the system, performing a certain unitary transformation and refermionizing it, we explicitly build corresponding quasiparticle operators and formulate a kinetic description in their terms. The latter describes, in particular, the sought density evolution.

The problem is characterized by a Hamiltonian $H = H_0 + H_{\text{int}}$, where the kinetic part H_0 describes two spinless chiral modes (labeled by subscript $\eta = R, L$ or, occasionally, $\eta = \pm 1$) with a non-linear spectrum

$$H_0 = \sum_{\eta, k} \eta k v_F : a_{\eta k}^\dagger a_{\eta k} : + (1/2m) \sum_{\eta, k} k^2 : a_{\eta k}^\dagger a_{\eta k} : . \quad (1)$$

The interaction part reads

$$H_{\text{int}} = (1/2) \int dx_1 dx_2 g(x_1 - x_2) \rho(x_1) \rho(x_2), \quad (2)$$

where $\rho = \rho_L + \rho_R$ is the density. The kinetic term can be bosonized as follows¹⁴

$$H_0 = \pi v_F \int dx (\rho_R^2 + \rho_L^2) + (4\pi^2/6m) \int (\rho_R^3 + \rho_L^3) \quad (3)$$

with Fourier components of the densities satisfying the standard commutation relations (L is the system length) $[\rho_{\eta, q}, \rho_{\eta', -q'}] = \eta \delta_{\eta, \eta'} \delta_{q, q'} L q / 2\pi$. The interaction mixes the chiral sectors. On the quadratic level, this coupling can be eliminated by a canonical transformation $R_q = U_2 \rho_{R, q} U_2^\dagger$, $L_q = U_2 \rho_{L, q} U_2^\dagger$ of the standard Bogoliubov form

$$\rho_{R, q} = \cosh \kappa_q R_q - \sinh \kappa_q L_q, \quad (4)$$

$$\rho_{L, q} = -\sinh \kappa_q R_q + \cosh \kappa_q L_q, \quad (5)$$

where $\tanh 2\kappa_q = g_q / (2\pi v_F + g_q)$. In terms of new fields, the quadratic part is

$$H^{(2)} = (\pi/L) \sum_q u_q (R_q R_{-q} + L_q L_{-q}), \quad (6)$$

with a sound velocity $u_q = v_F(1 + g_q/\pi v_F)^{1/2} = v_F/K_q$.

As a side effect of Bogoliubov transformation, the cubic part of the Hamiltonian acquires a form that mixes the right and left movers:

$$H^{(3)} = (2\pi^2/3mL^2) \sum_{\mathbf{q}} \Gamma_{\mathbf{q}} [(R_1 R_2 R_3 + L_1 L_2 L_3) + 3\Gamma'_{\mathbf{q}} (R_1 R_2 L_3 + L_1 L_2 R_3)]. \quad (7)$$

Here we have introduced notations $\mathbf{q} \equiv \{q_1, q_2, q_3\}$, $R_i = R_{q_i}$, $L_i = L_{q_i}$; the summation over \mathbf{q} is restricted to $q_1 + q_2 + q_3 = 0$ and we have defined vertices ($\kappa_i \equiv \kappa_{q_i}$)

$$\begin{aligned} \Gamma_{\mathbf{q}} &= \text{ch } \kappa_1 \text{ ch } \kappa_2 \text{ ch } \kappa_3 - \text{sh } \kappa_1 \text{ sh } \kappa_2 \text{ sh } \kappa_3, \\ \Gamma'_{\mathbf{q}} &= \text{sh } \kappa_1 \text{ sh } \kappa_2 \text{ ch } \kappa_3 - \text{ch } \kappa_1 \text{ ch } \kappa_2 \text{ sh } \kappa_3. \end{aligned} \quad (8)$$

The decoupling of the right and left sectors of the theory can be extended to the cubic level. To this end, we perform an additional unitary transformation $\tilde{\rho}_R = U_3 R U_3^\dagger$ and $\tilde{\rho}_L = U_3 L U_3^\dagger$, determined by the operator

$$U_3 = \exp \sum_{\mathbf{q}} [f_{\mathbf{q}} R_1 R_2 L_3 - (L \leftrightarrow R)], \quad (9)$$

where

$$f_{\mathbf{q}} = \frac{2\pi^2}{mL^2} \frac{\Gamma'_{\mathbf{q}}}{u_{q_1} q_1 + u_{q_2} q_2 - u_{q_3} q_3}. \quad (10)$$

After this transformation, the Hamiltonian H mixes the left and right modes only due to the terms quartic in the density

$$\begin{aligned} H &= (\pi/L) \sum_{\eta, q} u_q \tilde{\rho}_{\eta, q} \tilde{\rho}_{\eta, -q} \\ &+ (2\pi^2/3mL^2) \sum_{\eta, \mathbf{q}} \Gamma_{\mathbf{q}} \tilde{\rho}_{\eta, 1} \tilde{\rho}_{\eta, 2} \tilde{\rho}_{\eta, 3} + O(\tilde{\rho}^4). \end{aligned} \quad (11)$$

One can continue the procedure described above to disentangle the left and right movers order by order in perturbation theory in ρ/mv_F . This allows us to decouple the Hamiltonian into chiral sectors with an arbitrary accuracy. For our purposes, the transformations U_2 and U_3 are sufficient, and terms containing four and more density operators will be neglected.

We have thus obtained a chiral bosonic theory (11), with interaction originating from the non-linearity of the fermionic spectrum and a q -dependent sound velocity originating from the electron-electron interaction. We now proceed by refermionizing this theory, following the idea put forward in Ref.²⁶ (see also²¹), where such a mapping was performed after the conventional Bogoliubov transformation U_2 . It is crucial for our problem that we also carry out the transformation U_3 , decoupling the chiral sectors, and only then refermionize. More specifically, we define ‘‘composite fermion’’ operators that are built from the original ones by consecutive rotations

$$\tilde{\Psi}_\eta = U_3 U_2 \Psi_\eta U_2^\dagger U_3^\dagger. \quad (12)$$

Since the rotation is exponential in the density fields, this somewhat resembles the composite-fermion transformation in the fractional quantum Hall regime. In terms of the new operators, the Hamiltonian is given by

$$\begin{aligned} H &= \sum_{\eta, k} \tilde{\Psi}_{\eta, k}^\dagger \left(\eta u_0 k - \frac{k^2}{2m^*} \right) \tilde{\Psi}_{\eta, k} + \frac{1}{2L} \sum_{\eta, q} V_q \tilde{\rho}_{\eta, q} \tilde{\rho}_{\eta, -q} \\ &+ \frac{2\pi^2}{3mL^2} \sum_{\eta, \mathbf{q}} \gamma_{\mathbf{q}} \tilde{\rho}_{\eta, q_1} \tilde{\rho}_{\eta, q_2} \tilde{\rho}_{\eta, q_3}. \end{aligned} \quad (13)$$

The quadratic part of the Hamiltonian (13) is parametrized by the renormalized Fermi velocity $u_0 \equiv u_{q=0}$ and the spectral curvature

$$1/m^* \simeq \Gamma_{\mathbf{q}=0}/m. \quad (14)$$

There is also a residual interaction between particles represented by two-particle and three-particle vertices

$$V_q = 2\pi(u_q - u_0), \quad \gamma_{\mathbf{q}} = \Gamma_{\mathbf{q}} - \Gamma_{\mathbf{q}=0}. \quad (15)$$

The residual interaction V_q vanishes at low momenta, ($V_q \propto q^2$ for a generic finite-range interaction) and is irrelevant in the renormalization-group sense. The three body interaction is still weaker ($\gamma_{\mathbf{q}} \propto \mathbf{q}^2$ and, in addition, contains the factor $\rho/m^*u \ll 1$) and we neglect it from now on²⁷. The disappearance of the interaction at small momenta, makes perturbation theory for the composite fermions regular in the infrared limit, and the system behaves as a weakly interacting Fermi gas.

We define the quasiparticle density matrix

$$\begin{aligned} \tilde{f}_\eta(x, y, t) &= \langle \tilde{\Psi}_\eta^\dagger(x - y/2, t) \tilde{\Psi}_\eta(x + y/2, t) \rangle \\ &= \int (dp/2\pi) e^{ipy} f_\eta(x, p, t) \end{aligned} \quad (16)$$

that within the Hartree approximation satisfies the collisionless quantum kinetic equation

$$\begin{aligned} \partial_t \tilde{f}_\eta(p, x, t) + (p/m^*) \partial_x \tilde{f}_\eta(p, x, t) + \int (dp'/2\pi) e^{-ip'y} \\ \times \tilde{f}_\eta(x, y, t) [\tilde{\phi}_\eta(x + y/2) - \tilde{\phi}_\eta(x - y/2)] = 0, \end{aligned} \quad (17)$$

with the self-consistent electric field

$$\tilde{\phi}_\eta(x, t) = \int dx' V(x - x') \tilde{\rho}_\eta(x', t), \quad (18)$$

To obtain the physical density ρ out of the solution $\tilde{\rho}$ one needs to use the relation between the densities; in the leading order $\rho \simeq \sqrt{K} \tilde{\rho}$, Appendix A. Note that Eq. (17) is exact in the limits of non-interacting electrons and of a harmonic LL ($m \rightarrow \infty$, arbitrary electron interaction), see Appendix B.

In order to analyze the pulse dynamics, we solve Eq.(17) numerically (see Appendix C), focusing on times exceeding the "shock formation time" t_c when the phase space distribution of non-interacting fermions develops an inverse population. For initial density perturbation of the amplitude $\Delta\rho$ and spacial extent Δx one finds $t_c \sim m\Delta x/\Delta\rho$. The Wigner function in the initial state was discussed in Refs.^{24,28}, see also Appendix B. We plot it in Fig.1 for a gaussian density hump ($\tilde{\rho}_0(x) = \Delta\rho \exp(-x^2/2\sigma^2)$ with $\sigma = 200/mv_F$ and $\Delta\rho = 0.01mv_F$) in the initial state. Besides changing from 0 to 1 at classical Fermi surface $p_F(x) = 2\pi\tilde{\rho}_0(x)$, the Wigner function exhibits phase-space oscillations (that do not manifest themselves in the total density for a spatially smooth hump).

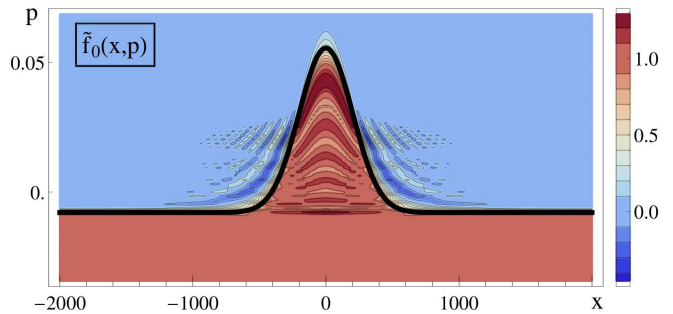


FIG. 1: The initial quasiparticle Wigner function $\tilde{f}_0(x, p)$. Thick black line shows the classical Fermi surface $p_F(x) = 2\pi\rho_0(x)$.

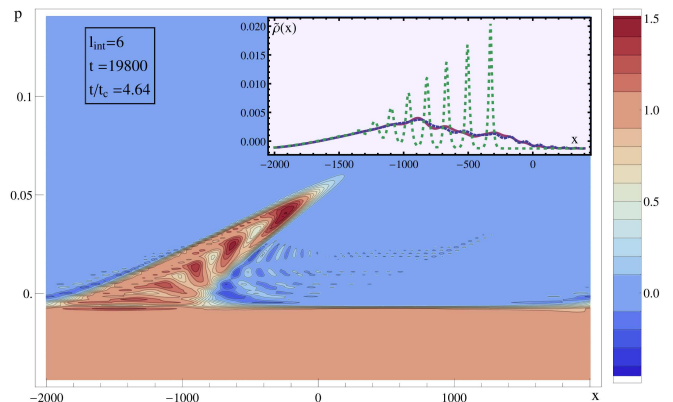


FIG. 2: Quasiparticle phase-space distribution (Wigner function) for a short interaction range, $l_{\text{int}} = 6/mv_F$, at $t = 4.6t_c$. Inset: corresponding density (solid red line) in comparison to the density of non-interacting fermions (green dotted) and the predictions of classical hydrodynamic theory (dashed blue).

While our approach is very general, we now focus on a model of finite range interaction

$$g(q) = (1/l_0 m) \exp(-q^2 l_{\text{int}}^2), \quad (19)$$

with two lengths l_0 and l_{int} parameterizing its strength and range. The classical hydrodynamics emerges if two conditions are fulfilled

$$l_0 \Delta\rho \ll 1, \quad l_{\text{int}}^2 \Delta\rho/l_0 \gg 1. \quad (20)$$

In the opposite limit (if at least one of the inequalities $l_0 \Delta\rho \gg 1$ and $l_{\text{int}}^2 \Delta\rho/l_0 \ll 1$ is fulfilled) the solution remains close to that for free fermions. To illustrate the behavior of the solution of the kinetic equation (17) in both regimes and in a crossover between them, we fix $l_0 = 1/mv_F$ and $\Delta\rho = 0.01mv_F$ such that the first of the conditions (20) is well fulfilled and vary l_{int} .

For a sufficiently short-range interaction, an inverse population develops for $t > t_c$. This is demonstrated in Fig. 2, where a snapshot of the phase space at time $t = 4.64t_c$ is shown for interaction range $l_{\text{int}} = 6/mv_F$. In this case the second parameter of Eq. (20) is relatively small, i.e. $l_{\text{int}}^2 \Delta\rho/l_0 = 0.36$. The inset shows the corresponding density in comparison to that of non-interacting

fermions and the predictions of hydrodynamic theory. As one sees, the interacting density is close to that of free fermions, meaning that the “composite fermion” interaction effects are weak, as expected. It should be emphasized that the original electron interaction may well be strong in this regime; i.e. the parameter $1/l_0mv_F$ does not need to be small. (In our modeling it is equal to unity and can also be larger.) As for free fermions, one observes oscillations of the total density that originate from the phase-space oscillations in the initial state and develop in the region where the inverse population is formed^{24,25}. We also provide a comparison with the density calculated by using a classical hydrodynamic equation (obtained as a saddle-point of the bosonic theory). Clearly, the classical hydrodynamics, which yields much stronger oscillations, is not a proper way to describe the system in this regime of weakly-interacting quasiparticles.

As the quasiparticle interaction becomes stronger ($l_{\text{int}} = 20/mv_F$), the density significantly deviates from the free fermion limit and the agreement with the hydrodynamics improves, see Fig.3. However, the system still shows clear traces of the population inversion leading to deviations from the hydrodynamic solution that proliferate with time and become quite substantial at $t = 4.6t_c$. In this intermediate regime neither free-fermion model nor hydrodynamic approximations are valid, and the kinetic approach is the only adequate tool to controllably address the problem.

With a further increase of the interaction strength ($l_{\text{int}} = 20/mv_F$) the agreement between hydrodynamic and kinetic approaches is reached, see Fig. 4. In this regime the phase space distribution is approximately given by a Fermi function with a position-dependent Fermi momentum $p_F(x)$, determined by the classical hydrodynamic equation. On top of sharp Fermi surface, we observe an additional “fine structure” in the phase-space distribution, shown in Fig. 4. It remains to be seen whether these details of the quantum state, which are beyond the hydrodynamic picture, lead to strong deviations from the hydrodynamic solution at the longer times.

In addition to the selfconsistent electric field, the quasiparticle interaction in Eq. (13) causes inelastic quasiparticle scattering. When taken into account, these processes generate a collision integral in the kinetic equation (17). Dominant contributions originate from triple collisions^{29–34} and from the $\tilde{\rho}^3$ term in Eq. (13). A quick estimate shows that the rate $1/\tau_{\text{in}}$ of such processes is proportional to a high-power of a small parameter $\Delta\rho/mv_F$ (or of T/mv_F at finite temperature T) and is thus very small. Therefore there is a parametrically broad range of times, $t < \tau_{\text{in}}$, for which the collisionless kinetic equation studied in this work is applicable. A detailed analysis of the inelastic relaxation leading to a viscous hydrodynamics at $t > \tau_{\text{in}}$ will be presented elsewhere.

To summarize, we have studied evolution of a density pulse of 1D interacting fermions with a non-linear single-particle spectrum. We identified excitations that

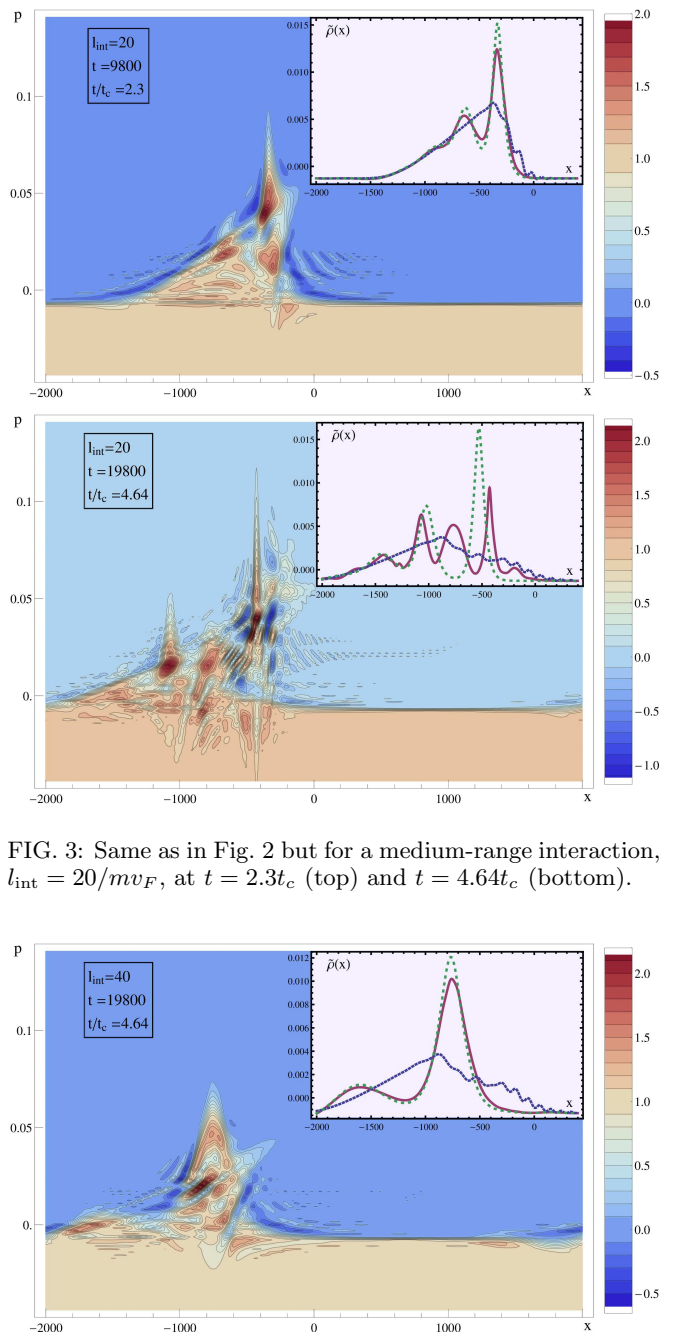


FIG. 3: Same as in Fig. 2 but for a medium-range interaction, $l_{\text{int}} = 20/mv_F$, at $t = 2.3t_c$ (top) and $t = 4.64t_c$ (bottom).

FIG. 4: Same as in Fig. 2 but for a long-range interaction, $l_{\text{int}} = 40/mv_F$, at time $t = 4.6t_c$.

play a role of weakly interacting quasiparticles for non-equilibrium phenomena inside the wire and described their dynamics by a quantum kinetic equation. The evolution of the corresponding phase space distribution is determined by two competing effects: the dispersion that tends to overturn Fermi surface, and the quasiparticle interaction that tends to stabilize it. Solving numerically the kinetic equation, we have demonstrated a crossover from the free-fermion-like evolution for weak or short-range interaction to hydrodynamics emerging in the case

of sufficiently strong, long-range interaction.

Our work shows that while 1D interacting systems are not Fermi liquids in the conventional sense, kinetic phenomena in such systems can be cast into Landau paradigm of weakly interacting fermionic quasiparticles. We foresee numerous extensions and applications of our formalism, including other types of interaction, relax-

ation phenomena (also in presence of disorder), and edge states of integer and fractional quantum Hall systems and topological insulators.

We acknowledge discussions with I.V.Gornyi and support by Alexander von Humboldt Foundation, ISF, and GIF.

Appendix A: Physical density vs. density of composite fermions

In this section we write down explicit expressions for the physical densities ρ_η in terms of the densities of composite fermions. The decoupling of the left and right-movers in the quadratic Hamiltonian $H^{(2)}$ (see Eq.(6) of the main text) is achieved via the Bogolubov transformation

$$\rho_{R,q} = U_2^+ R_q U_2 = \cosh \kappa_q R_q - \sinh \kappa_q L_q, \quad (\text{A1})$$

$$\rho_{L,q} = U_2^+ L_q U_2 = -\sinh \kappa_q R_q + \cosh \kappa_q L_q. \quad (\text{A2})$$

To perform decoupling of the cubic terms one needs to perform the non-linear rotation

$$R = U_3^+ \tilde{\rho}_R U_3, \quad L = U_3^+ \tilde{\rho}_L U_3, \quad (\text{A3})$$

with

$$U_3 = \exp \left(\sum_{\mathbf{q}} f_{\mathbf{q}} R_1 R_2 L_3 - (L \leftrightarrow R) \right), \quad (\text{A4})$$

$$f_{\mathbf{q}} = \frac{2\pi^2}{mL^2} \frac{\Gamma'_{\mathbf{q}}}{u_1 q_1 + u_2 q_2 - u_3 q_3}. \quad (\text{A5})$$

To third order in densities we obtain

$$R_q = \tilde{\rho}_{Rq} + \frac{qL}{\pi} \sum_{2+3-q=0} f_{(-q,2,3)} \tilde{\rho}_{R2} \tilde{\rho}_{L3} - \frac{qL}{2\pi} \sum_{1+2-q=0} f_{(1,2,-q)} \tilde{\rho}_{L1} \tilde{\rho}_{L2}, \quad (\text{A6})$$

$$L_q = \tilde{\rho}_{Lq} + \frac{qL}{\pi} \sum_{2+3-q=0} f_{(-q,2,3)} \tilde{\rho}_{L2} \tilde{\rho}_{R3} - \frac{qL}{2\pi} \sum_{1+2-q=0} f_{(1,2,-q)} \tilde{\rho}_{R1} \tilde{\rho}_{R2}. \quad (\text{A7})$$

The connection of ρ_η and $\tilde{\rho}_\eta$ can be now read off from (A1), (A6) and (A7).

The consideration above simplifies considerably when the relevant spacial scale of the density variation is small compared to the interaction radius. In this case the transformations U_2 and U_3 act locally in space leading to

$$\rho_R(x) = \frac{\sqrt{K_0}}{2} (R(x) + L(x)) + \frac{1}{2\sqrt{K_0}} (R(x) - L(x)), \quad (\text{A8})$$

$$\rho_L(x) = \frac{\sqrt{K_0}}{2} (R(x) + L(x)) - \frac{1}{2\sqrt{K_0}} (R(x) - L(x)), \quad (\text{A9})$$

and

$$R(x) = \tilde{\rho}_R(x) + \frac{\pi}{m} \frac{1 - K_0^2}{8u_0\sqrt{K_0}} \left[-\frac{1}{\pi} \partial_x (\tilde{\rho}_R(x) \tilde{\varphi}_L(x)) + \tilde{\rho}_L^2(x) \right], \quad (\text{A10})$$

$$L(x) = \tilde{\rho}_L(x) + \frac{\pi}{m} \frac{1 - K_0^2}{8u_0\sqrt{K_0}} \left[\frac{1}{\pi} \partial_x (\tilde{\rho}_L(x) \tilde{\varphi}_R(x)) + \tilde{\rho}_R^2(x) \right]. \quad (\text{A11})$$

Here $\tilde{\varphi}_\eta(x)$ is defined by the usual relation

$$\tilde{\rho}_\eta(x) = \frac{\eta}{2\pi} \partial_x \tilde{\varphi}_\eta(x). \quad (\text{A12})$$

In the leading order in ρ/mv_F the physical density $\rho(x) = \rho_L + \rho_R \simeq \sqrt{K_0} (\tilde{\rho}_R + \tilde{\rho}_L)$.

Appendix B: Kinetic equation and chiral hydrodynamics

We now discuss the relation between the kinetic approach, developed above and hydrodynamics description for 1D fermions with generic finite range interaction, developed in Ref.²⁴.

In terms of the bosonic densities the Hamiltonian of the system can be written as [see main text, Eq. (13)]

$$H = \sum_{\eta} \int dx \left[\pi u_0 \hat{\rho}_{\eta}^2 + \frac{2\pi^2}{3m^*} \hat{\rho}_{\eta}^3 \right] + \frac{1}{2} \int dx dx' \tilde{\rho}_{\eta}(x) V(x-x') \tilde{\rho}_{\eta}(x'), \quad (\text{B1})$$

where we approximate the interaction vertex $\Gamma_{\mathbf{q}} \simeq \Gamma_{\mathbf{q}=0}$ and use real space representation.

The operators of chiral density components satisfy Heisenberg equation

$$\partial_t \hat{\rho}_{\eta} + \eta \left(u_0 + \frac{2\pi}{m^*} \hat{\rho}_{\eta} \right) \partial_x \hat{\rho}_{\eta} + \frac{\eta}{2\pi} \int dx' V(x-x') \partial_{x'} \hat{\rho}_{\eta}(x') = 0. \quad (\text{B2})$$

In the classic limit the operators in Eq. (B2) are replaced by the real density field. By ignoring the difference between density operators and their expectation values one neglects the quantum loop corrections to the classical equations of motion. Such corrections play an important role in evolution of the density field Ref.²⁴, in particular in the region where hydrodynamic equations develop instabilities (and phase space of quasi-particle acquires an inverse population). Sufficiently strong electron interaction prevents the emerging instabilities in hydrodynamic theory, which allows to neglect the loop corrections in a controlled way. For the case of finite range interaction

$$g(q) = \frac{1}{l_0 m} e^{-q^2 l_{\text{int}}^2} \quad (\text{B3})$$

the hydrodynamics is justified, provided that

$$\sqrt{\frac{l_{\text{int}}^2 \Delta\rho}{l_0}} \gg 1 \quad \text{and} \quad l_0 \Delta\rho \ll 1. \quad (\text{B4})$$

Here $\Delta\rho$ is the amplitude of the density perturbation in the initial state.

The classic hydrodynamic theory can be straightforwardly derived from the kinetic description of the main text. For the right-moving particles (from now on we focus on this case and omit the chirality index η) the kinetic equation reads

$$\partial_t \tilde{f}(p, x, t) + \left(u_0 + \frac{p}{m^*} \right) \partial_x \tilde{f}(p, x, t) + \int \frac{dp}{2\pi} e^{-ipy} \tilde{f}(x, y, t) \left[\tilde{\phi} \left(x + \frac{y}{2} \right) - \tilde{\phi} \left(x - \frac{y}{2} \right) \right] = 0, \quad (\text{B5})$$

$$\phi(x, t) = \int dx' V(x-x') \tilde{\rho}(x', t). \quad (\text{B6})$$

The equation (B5) should be supplied with the initial conditions $\tilde{f}_0(x, p)$, that needs to be calculated separately. As in the main text, we assume that the perturbation in electronic density is created by the applying the smooth external potential $U(x)$ to the uniform Fermi sea. In this case the curvature of electronic spectrum has little effect on the initial Wigner function, and the standard bosonization technique enables us to find $\tilde{f}_0(x, p)$. In the vicinity of the right Fermi point (cf. discussion of the Wigner function for non-interacting fermions in Ref.²⁴) the Wigner function can be written as

$$\tilde{f}_0(x, p) = \int \frac{dy}{2\pi i(y-i0)} \exp \left[-ipy + 2\pi i \int_{x_-}^{x_+} \tilde{\rho}_0(x') dx' \right], \quad x_{\pm} \equiv x \pm \frac{y}{2}, \quad (\text{B7})$$

where $\tilde{\rho}_0(x)$ is the expectation value of fermionic density in the external potential $U(x)$. We note, that the details of the interaction are encoded in the static Wigner function only through $\tilde{\rho}_0$. Several simple facts about equation (B5) help to clarify its connection to hydrodynamics.

In the limit ($m^* = \infty$) Eq. (B5) yields

$$\tilde{f}(x, p, t) = \int \frac{dy}{2\pi i(y-i0)} \exp \left[-ipy + 2\pi i \int_{x_-}^{x_+} \tilde{\rho}(x', t) dx' \right]. \quad (\text{B8})$$

This corresponds to density evolution

$$\partial_t \tilde{\rho} + u_0 \partial_x \tilde{\rho} + \frac{1}{2\pi} \int dx' V(x-x') \partial_{x'} \tilde{\rho}(x') = 0 \quad (\text{B9})$$

in accordance with harmonic LL model. As expected, Eq.(B5) is exact in the limit $m \rightarrow \infty$.

Performing the gradient expansion in Eq.(B5) one obtains the standard Boltzmann equation

$$\partial_t \tilde{f}(p, x, t) + \left(u_0 + \frac{p}{m^*}\right) \partial_x \tilde{f}(p, x, t) - \partial_x \phi(x) \partial_p \tilde{f}(p, x, t) = 0. \quad (\text{B10})$$

Approximating the initial condition (B7) by

$$\tilde{f}_0(x, p) = \Theta(2\pi\tilde{\rho}_0(x) - p). \quad (\text{B11})$$

one finds the formal solution of Eq. (B10)

$$\tilde{f}(x, p, t) = \Theta(2\pi\rho(x, t) - p), \quad (\text{B12})$$

where the density $\rho(x, t)$ satisfies the hydrodynamic equation (B2).

Appendix C: Numerical solution of the kinetic equation

In this section we briefly discuss the algorithm used for numeric simulation of Eq. (B5). We use the model of fermions on a ring, of the circumference L_x . This induces periodic boundary conditions for the Wigner function $f(x, y)$ with the period with period $L_y = 2L_x$, as a function of y and x correspondingly. The fermionic momentum p in $f(x, p)$ is quantized in units of $2\pi/L_y$, while the momentum q conjugate to x is quantized in units of $2\pi/L_x$. To perform numerical simulations we impose the cut-off $2\pi N_x/L_x$ and $2\pi N_y/L_y$ for momenta q and p respectively. In our calculations, the values of the parameters $L_x = 4000$ (in units where $\lambda_F \equiv mV_F = 2\pi$), $N_x \sim 2500$ and $N_y \sim 500$ were used. We checked that the final results are stable with respect to the variation of these parameters. We model the initial density bump by a Gaussian with the dispersion $\sigma = 200$ that contain $N \approx 5$ particles.

Periodic boundary conditions enable the use of fast Fourier transform algorithm for the calculation of $\partial_t \tilde{f}$, given by (B5). Combined with the standard fourth-order Runge-Kutta time stepper this provides us with the fast and accurate algorithm for the numerical solution of Eq. (B5).

-
- ¹ L.D. Landau, Sov. Phys. JETP **3**, 920 (1957).
² E.M. Lifshitz, and L.P. Pitaevskii, *Statistical Physics* (Part 2) (Elsevier, 1980).
³ L.P. Kadanoff and G. Baym, *Quantum Statistical Mechanics* (Benjamin, 1962).
⁴ M. Stone, *Bosonization* (World Scientific, 1994).
⁵ J. von Delft and H. Schoeller, Annalen Phys. **7**, 225 (1998).
⁶ A.O. Gogolin, A.A. Nersesyan, and A.M. Tsvelik, *Bosonization in Strongly Correlated Systems*, (University Press, Cambridge 1998).
⁷ T. Giamarchi, *Quantum Physics in One Dimension*, (Claverdon Press Oxford, 2004).
⁸ D.L. Maslov, in *Nanophysics: Coherence and Transport*, edited by H. Bouchiat, Y. Gefen, G. Montambaux, and J. Dalibard (Elsevier, 2005), p.1.
⁹ I. V. Protopopov, D. B. Gutman, and A. D. Mirlin Phys. Rev. Lett. **110**, 216404 (2013); Lith. J. Phys. **52**, 165 (2012).
¹⁰ D.B. Gutman, Yuval Gefen, A.D. Mirlin J. Phys. A: Math. Theor. **44** 165003 (2011); Phys. Rev. B **81**, 085436 (2010).
¹¹ I. Bloch, J. Dalibard, and W. Zwerger, Rev. Mod. Phys. **80**, 885 (2008).
¹² T. Lahaye, C. Menotti, L. Santos, M. Lewenstein, and T. Pfau, Rep. Prog. Phys. **72**, 126401 (2009).
¹³ E. Bettelheim, A.G. Abanov, and P. Wiegmann, Phys. Rev. Lett. **97**, 246401 (2006).
¹⁴ M. Schick, Phys. Rev. **166**, 404 (1968).
¹⁵ A. Jevicki and B. Sakita, Nuc. Phys. B **165**, 511 (1980).
¹⁶ F.D.M. Haldane, Phys. Rev. Lett. **47**, 1840 (1981).
¹⁷ B. Sakita, *Quantum Theory of Many-variable Systems and Fields* (Wolrd Scientific, Singapore, 1985).
¹⁸ A. P. Polychronakos, Phys.Rev.Lett. **74**, 5153 (1995).
¹⁹ A.G. Abanov and P. Wiegmann, Phys. Rev. Lett. **95**, 076402 (2005).
²⁰ M. Stone, I. Anduaga and L. Xing, J. Phys. A: Math. Theor. **41**, 275401 (2008).
²¹ A. Imambekov and L.I. Glazman, Science **323**, 228 (2009); Phys. Rev. Lett. **102**, 126405 (2009).

- ²² A. Imambekov, T.L. Schmidt, and L.I. Glazman, *Rev. Mod. Phys* **84**, 1253 (2012).
- ²³ D.N. Aristov, *Phys. Rev. B* **76**, 085327 (2007).
- ²⁴ I. V. Protopopov, D. B. Gutman, P. Schmitteckert, and A. D. Mirlin, *Phys. Rev. B* **87**, 045112 (2013) .
- ²⁵ E. Bettelheim and L.I. Glazman, *Phys. Rev. Lett.* **109**, 260602, 2012.
- ²⁶ A.V. Rozhkov, *Phys. Rev. B* **77**, 125109 (2008); *Phys. Rev. B* **74**, 245123 (2006); *Eur.Phys.J.* **47** , 193 (2005).
- ²⁷ The three body interaction turns out to be important for the calculation of the inelastic relaxation time and will be discussed in details in the separate publication.
- ²⁸ E. Bettelheim, P. B. Wiegmann, *Phys. Rev. B* **84** 085102 (2011).
- ²⁹ M. Khodas, M. Pustilnik, A. Kamenev, and L.I. Glazman, *Phys. Rev. B* **76**, 155402 (2007).
- ³⁰ A.M. Lunde, K. Flensberg, and L. I. Glazman, *Phys. Rev. B* **75**, 245418 (2007).
- ³¹ T. Karzig, L.I. Glazman, and F. von Oppen, *Phys. Rev. Lett.* **105**, 226407 (2010).
- ³² Z. Ristivojevic, and K. A. Matveev, *Phys. Rev. B* **87**, 165108 (2013).
- ³³ T. Micklitz, A. Levchenko, and A. Rosch, *Phys. Rev. Lett.* **109**, 036405 (2012).
- ³⁴ A. P. Dmitriev, I. V. Gornyi, and D. G. Polyakov *Phys. Rev. B* **86**, 245402 (2012).